

Original Article

## Two stages segmentation for Leaf Area Index estimation using digital cover photography

Segmentação em duas para estimativa do Índice de Área Foliar utilizando fotografia digital de cobertura

A. B. Raharjo<sup>a</sup> , F. W. Edlim<sup>a</sup> , D. Sunaryono<sup>a</sup> , S. I. Sabilla<sup>b</sup>  and M. Muryono<sup>c</sup> 

<sup>a</sup>Institut Teknologi Sepuluh Nopember, Department of Informatics, Surabaya, Indonesia

<sup>b</sup>Institut Teknologi Sepuluh Nopember, Department of Medical Technology, Surabaya, Indonesia

<sup>c</sup>Institut Teknologi Sepuluh Nopember, Department of Biology, Surabaya, Indonesia

### Abstract

Leaf Area Index (LAI) is the ratio of ground surface area covered by leaves. LAI plays a significant role in the structural characteristics of forest ecosystems. Therefore, an accurate estimation process is needed. One method for estimating LAI is using Digital Cover Photography. However, most applications for processing LAI using digital photos do not consider the brown color of plant parts. Previous research, which includes brown color as part of the calculation, potentially produced biased results by the increased pixel count from the original photo. This study aims to enhance the accuracy of LAI estimation. The proposed methods consider the brown color while minimizing errors. Image processing is carried out in two stages to separate leaves and non-leaf pixels by using the RGB color model for the first stage and applying the CIELAB color model in the second stage. Proposed methods and existing applications are evaluated against the actual LAI value obtained using Terrestrial Laser Scanning (TLS) as the ground truth. The results demonstrate that the proposed methods effectively identify non-leaf parts and exhibit the lowest error rates compared to other methods. In conclusion, this study provides alternative techniques to enhance the accuracy of LAI estimation in forest ecosystems.

**Keywords:** CIELAB color, digital cover photography, Leaf Area Index, forestry.

### Resumo

O Índice de Área Foliar (IAF) é a razão da área da superfície do solo coberta por folhas. O IAF desempenha um papel significativo nas características estruturais dos ecossistemas florestais. Portanto, é necessário um processo de estimativa preciso. Um método para estimar o IAF é o uso da Fotografia de Cobertura Digital. No entanto, a maioria das aplicações para processamento do IAF usando fotos digitais não considera a cor marrom das partes das plantas. Pesquisas anteriores, que incluem a cor marrom no cálculo, potencialmente produziram resultados enviesados devido ao aumento na contagem de pixels da foto original. Este estudo tem como objetivo aprimorar a precisão da estimativa do IAF. Os métodos propostos consideram a cor marrom enquanto minimizam erros. O processamento de imagem é realizado em duas etapas para separar os pixels de folhas e não folhas, usando o modelo de cor RGB na primeira etapa e aplicando o modelo de cor CIELAB na segunda etapa. Os métodos propostos e as aplicações existentes são avaliados em relação ao valor real do IAF obtido por meio da Varredura a Laser Terrestre (TLS) como referência. Os resultados demonstram que os métodos propostos identificam efetivamente as partes não foliares e apresentam as menores taxas de erro em comparação com outros métodos. Concluindo, este estudo oferece técnicas alternativas para aprimorar a precisão da estimativa do IAF em ecossistemas florestais.

**Palavras-chave:** Cor CIELAB, fotografia digital de cobertura, Índice de Área Foliar, silvicultura.

## 1. Introduction

Modeling plant growth and water consumption in forests is essential in determining productivity and the interaction between the soil and the forest atmosphere, both physical and biophysical (Smagin et al., 2023). Two processes that can be used to model growth are evapotranspiration and tree photosynthesis. The soil level covered by leaves, the

Leaf Area Index (LAI), greatly influences those two processes (Nomura et al., 2020). LAI is defined as the single side area of leaves per land area (Parker, 2020). It is also needed for validating plant architectural models (Rani et al., 2016). Ecosystem models simulate LAI as a key determinant as the amount of light intercepted by the canopy influences

\*e-mail: agus.budi@its.ac.id

Received: October 25, 2023 – Accepted: April 25, 2024



This is an Open Access article distributed under the terms of the Creative Commons Attribution License, which permits unrestricted use, distribution, and reproduction in any medium, provided the original work is properly cited.

net primary production (Stuart-Haëntjens et al., 2015). At global distribution, LAI provides an empirical basis for the effects of global climate change.

The estimation of Leaf Area Index (LAI) can be accomplished through direct and indirect methods. Direct estimation involves defoliation of the canopy or visual observation, where the observer looks up vertically and records whether the canopy obstructs the view of the sky (Jennings et al., 1999). However, such observational methods may introduce errors if not conducted entirely vertically. To aid in accurate observation, a Densitometer (Johansson, 1985), can be utilized, which comprises a 45-degree mirror and two spirit levels—one in the horizontal direction and one in the vertical direction. This instrument facilitates observation as close to vertical as possible. Furthermore, specialized instruments designed for LAI calculation are available. One example is the Li-Cor-2000. Nonetheless, the Li-Cor-2000 has certain limitations, including suboptimal performance in LAI determination (Casa et al., 2019) and high cost (Chianucci and Cutini, 2012).

The indirect method is carried out by utilizing digital cameras. One such method is Digital Hemispherical Photography (DHP) which uses cameras with fisheye lenses. However, this method also has some drawbacks, where the result is susceptible to the exposure of the camera (Beckschäfer et al., 2013), gamma correction (Chianucci and Cutini, 2012), and the image processing method used (Liu et al., 2021). Another indirect method is Digital Cover Photography (DCP), which is much faster, can be easily automated, is cheap, and is readily available using a regular camera compared to the special lenses that are needed for DHP (Chianucci and Cutini, 2012; Fuentes et al., 2008; Chianucci, 2015; Alivernini et al., 2018).

Several readily available applications can estimate LAI from digital cover images. Examples include VitiCanopy (De Bei et al., 2016), CaCo (Alivernini et al., 2018), and coverR (Chianucci et al., 2022). While VitiCanopy is designed specifically for grapevines, it does not consider the brown color of tree branches, leaves, and trunks. A method proposed by Mora et al. (2016), which considers brown color using a two-step segmentation, has limitations addressed in this study. The improvement is evaluated using a dataset of Gap Fraction and LAI from *Fagus sylvatica L.*

This research aims to integrate the proposed Leaf Area Index (LAI) calculation method with a web-based information system, offering a valuable service for LAI estimation. This integration holds significant potential for enhancing forest ecosystem monitoring and conservation policies. By improving the efficiency and accuracy of LAI estimation, the initiative can provide valuable insights into canopy structure, biomass distribution, and overall forest health. This enhanced understanding of ecosystem dynamics, including carbon cycling and species composition, can inform more effective land management and conservation strategies. Moreover, the stream-lined LAI estimation process reduces the need for manual observations, enabling more scalable monitoring efforts to detect environmental changes and implement timely interventions. Additionally, the integration of innovative LAI estimation methods contributes to advancements in remote sensing and ecosystem modeling, benefiting

various scientific disciplines. Ultimately, this initiative aims to support evidence-based policymaking and promote the sustainable management of forest resources, aligning environmental conservation with socioeconomic development goals.

## 2. Materials and Methods

### 2.1. Materials

The dataset used in this research consists of 315 images of the *Fagus sylvatica L.* species obtained from seven locations in Italy. Previous studies (Chianucci, 2015; Chianucci et al., 2022) have effectively utilized same datasets in their analyses, thus affirming the adequacy of this dataset for the current research objectives. The 315 images offer comprehensive coverage and variability, enabling the capture of diverse canopy structures across the seven locations. Each location comprises nine observation areas, resulting in a total of 63 observation areas. Within each observation area, five pictures are taken alongside one TLS observation to derive Gap Fraction and Leaf Area Index values. Specifically, one picture is captured at the same point as the TLS observation, while the remaining four are taken five meters apart from the initial picture, aligned with the cardinal directions, as illustrated in Figure 1.

### 2.2. Method

This research is constructed based on the previous method proposed by Mora et al. which utilizes a two-step segmentation process to separate non leaf elements (Mora et al., 2016). The first segmentation takes the blue channel of an RGB image with  $x \times y$  pixel size. Then a process to determine a threshold value is done automatically using Otsu Algorithm (Xu et al, 2011), resulting in a value ( $O_t$ ). This value is then used to separate pixels representing sky and vegetation. For each pixel from the blue channel, if the

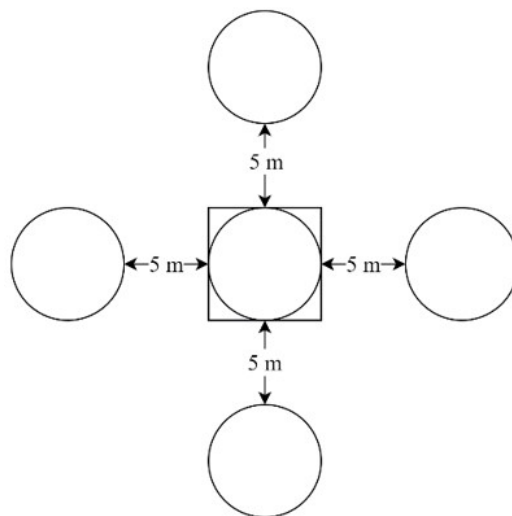


**Figure 1.** Data acquisition position for TLS (square) and Cover Images (circle).

value is larger than the threshold value ( $O_t$ ), then that pixel will be categorized as sky pixel as shown in Equation 1.

$$If_{ij} = \begin{cases} 1, & B_{ij} > O_t \\ 0, & B_{ij} \leq O_t \end{cases} \quad (1)$$

After categorizing each pixel in the images, the number of sky pixels can be evaluated. The evaluation is done by first dividing the image into subdivisions, as shown in Figure 2. The number of pixels representing skies and vegetation will be calculated for each subdivision. If the ratio between the skies pixel and vegetation pixel is more than 70%, then the number of sky pixels in that subdivision will be added to the total of large gaps ( $g_L$ ) and the total of gaps ( $g_T$ ). If not, the amount will be added to  $g_T$  only (Fuentes et al., 2008).

For the second segmentation, a color space conversion from RGB color space will be converted to CIELAB color space. This conversion process is carried out with the aim of separating pixels that represent non-leaf parts. For each pixel from the converted image a binarization is carried out. If the value from the  $a^*$  channel for that pixel ( $A_{ij}$ ) is not 0 then the result for the second segmentation for that pixel ( $Is_{ij}$ ) represents the non-leaf part using Equation 2.

$$Is_{ij} = \begin{cases} 1, & A_{ij} > 0 \\ 0, & A_{ij} \leq 0 \end{cases} \quad (2)$$

The first and second segmentation results will be used to calculate the number of pixels representing the leaf part only. This will result in a Leaf Area Index value that excludes the brown color part. The amount of wood in

the image, canopy cover ( $C_c$ ), and foliage cover ( $F_c$ ) can be calculated using the Equations 3, 4, and 5 respectively (Mora et al., 2016).

$$wood = \sum_i^x \sum_j^y Is_{ij} - \sum_i^x \sum_j^y If_{ij} = \sum_i^x \sum_j^y (Is_{ij} - If_{ij}) \quad (3)$$

$$C_c = 1 - \frac{gL}{p_T - wood} \quad (4)$$

$$F_c = 1 - \frac{g_T}{p_T - wood} = 1 - GF \quad (5)$$

From the canopy cover and foliage cover, the crown porosity ( $\phi$ ), clumping index ( $CI$ ), LAI, and effective LAI ( $LAI_e$ ) can be calculated by using Equations 6, 7, 8 and 9 respectively (MacFarlane et al., 2007; Chianucci et al., 2022).

$$\phi = 1 - \frac{F_c}{C_c} \quad (6)$$

$$CI = \frac{(1 - \phi) \ln(1 - F_c)}{\ln(\phi) F_c} \quad (7)$$

$$LAI = -f_c \frac{\ln(\phi)}{k} \quad (8)$$

$$LAI_e = LAI \cdot CI \quad (9)$$

Mora's method has some limitations in some instances. For example, in Figure 3a, the number of white pixels from the first segmentation is more significant than the number of white pixels compared to the second segmentation



Figure 2. Image subdivisions to  $n \times n$  grid.

(Figure 3b). According to (3), this will produce the value of *wood* to be negative. Contrary to the main goal, which is to eliminate pixels that are not leaves, the negative value causes the total number of pixels to increase, which causes the resulting fraction to be smaller. So, this study proposes changes in which the calculation of the value of *wood* is calculated using Equations 10 and 11.

$$wood = \sum_i^n \sum_j^m f(I_{fij}, I_{sij}) \tag{10}$$

$$f(I_{fij}, I_{sij}) = \begin{cases} 1, & \text{If } I_{fij} = 0, I_{sij} = 1 \\ 0, & \text{else} \end{cases} \tag{11}$$

This change is performed to prevent the occurrence of negative wood values in the case mentioned earlier. In addition, modifications are made in determining the threshold value. The previous method determined the threshold value between large and small gaps by dividing the image into several sub-image parts. In the example of Figure 4, the gap in the upper right corner will be divided into several sub-image parts. That will result in some parts of the gap being categorized as small gaps, as illustrated in Figure 4. To prevent that, a new threshold value between large and small gaps (*Lgt*) is set to 1.3% of the total image size (Macfarlane et al., 2007). If a gap has pixels count greater than *Lgt*, then the pixel count is added to *g<sub>L</sub>* and *g<sub>T</sub>*. Otherwise, it will be added to *g<sub>T</sub>* only.

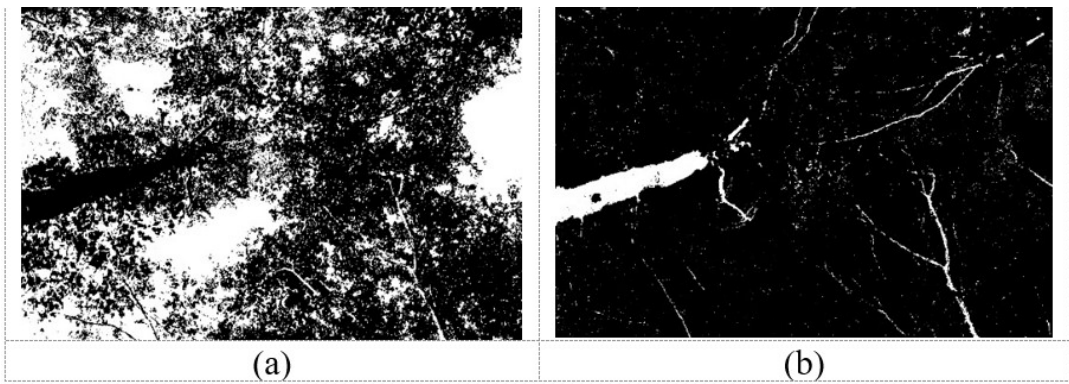


Figure 3. (a) first segmentation result, (b) second segmentation result.

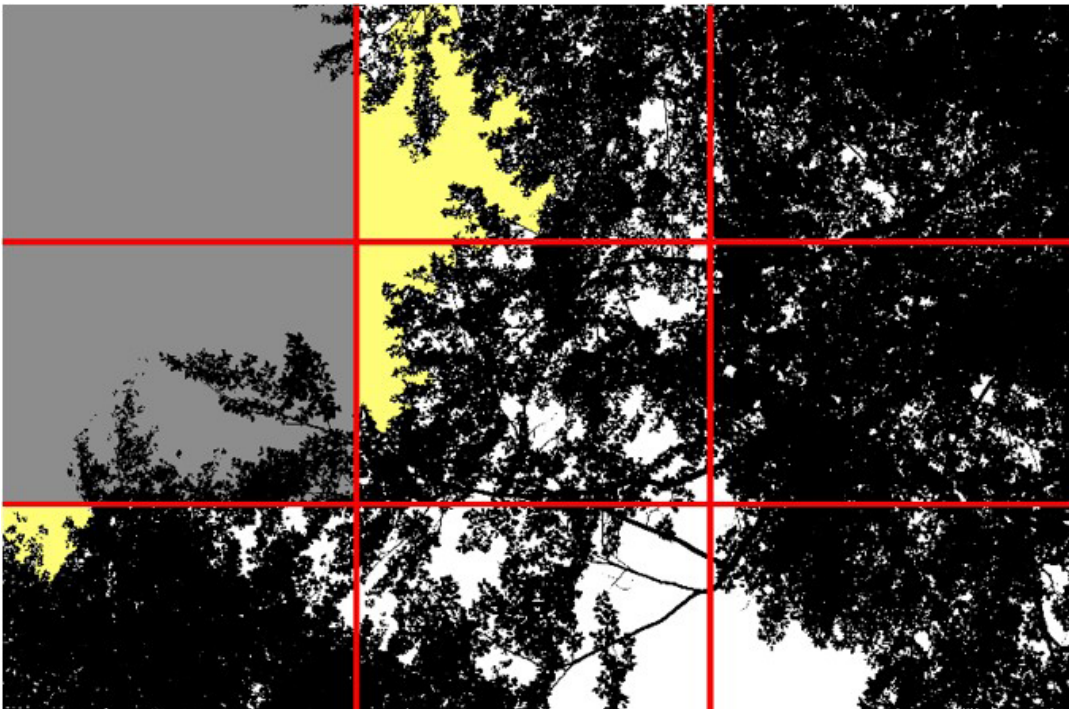


Figure 4. Parts of the same gap are considered as large gaps (grey) and small gaps (yellow).

The method proposed above will be referred to as Version 0. There are several further variations of Version 0, including:

### 2.2.1. Version 1: second-stage segmentation with a white gap size filter

Before calculating the value, the results of the second-stage segmentation will be filtered to reduce the number of small pixel clusters below a specific threshold value. This is done because the results of the second-stage segmentation often classify dry leaves as non-leaves due to their brown color, which should still be considered as leaves. A threshold value of 10 pixels will be tested to reduce the amount of misclassified dry leaves but also but not high enough to misclassify wood element as leaf. For example, in Figure 5b, which is the results from the second-stage segmentation of Figure 5a, many minor white points represent dry leaves. The filtering process will produce Figure 5c. It shows that in the filtered second segmentation the amount of small white area is reduced.

### 2.2.2. Version 2: assuming non-leaves parts as gaps

In this version, the results of the two segmentation stages will be combined by looking at each pixel in both stages using a truth table as shown in Table 1. This is done to eliminate the need for calculating the *wood* value (3) by using the second stage segmentation as validation check for the first stage segmentation result. The validation check if a pixel is not a gap (black) in the first stage (Figure 6a) and not a leaf (white) in the second stage (Figure 6b). It will be considered as a gap (white). The resulting combination (Figure 6c) will then be used for calculation. The large gaps

( $g_L$ ) and total gaps ( $g_T$ ) are calculated using the combined result image rather from the first stage segmentation image.

### 2.2.3. Version 3: assuming non-leaves parts as non-gaps

In this method, the opposite of Version 2 is applied using truth table shown in Table 2, where if a pixel is a gap (white) in the first stage (Figure 6a) and not a leaf (white) in the second stage (Figure 6b). It will be considered a non-gap (black), as shown in Figure 7. Both version 2 and version 3 use the same pseudocode.

**Table 1.** Truth table for Version 2.

$I_{f_{ij}}$	$I_{s_{ij}}$	Combination Result
Black	Black	Black
Black	White	White
White	Black	White
White	White	White

**Table 2.** Truth table for Version 3.

$I_{f_{ij}}$	$I_{s_{ij}}$	Combination Result
Black	Black	Black
Black	White	Black
White	Black	White
White	White	Black

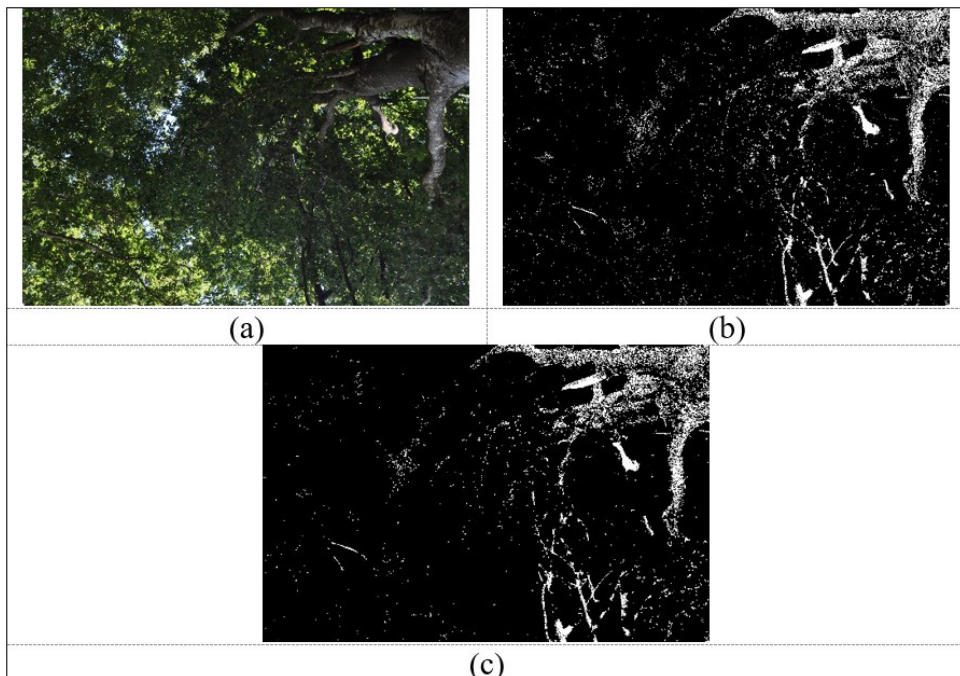


**Figure 5.** Example image for Version 1 : (a) input image, (b) second stage segmentation result, (c) filtered second stage segmentation result.

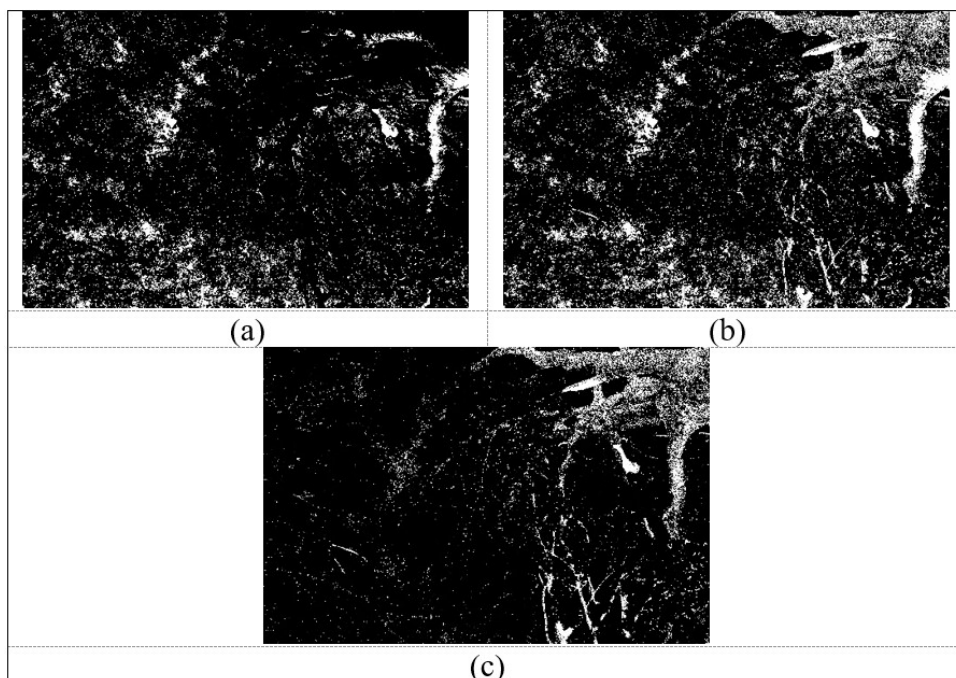


**Figure 6.** Example image for Version 2 : (a) first stage segmentation result, (b) second stage segmentation result, (c) combined result.

In each proposed method, at each observation area, one Gap Fraction (GF) value will be calculated using (5) from a photo taken at the same position as the TLS instrument, and 5 effective LAI estimates ( $LAI_e$ ) using (9) from five photos available at each observation area. The five LAI estimates will then be averaged and compared to the LAI estimate value from the TLS instrument. As a comparison, the same dataset will also be estimated using the methods proposed by (Mora et al., 2016), CaCo (Alivernini et al., 2018), available on GitHub, and coverR (Chianucci et al., 2022), accessible on GitLab. For the Mora et al. and CaCo methods, testing will not use the dataset used by the authors of the respective method. Furthermore, due to the absence of source code or available applications for testing the Mora's method, a program was created using the method described by Mora et al., 2016 in their publication (Mora et al., 2016). All methods will be tested using an extinction coefficient value ( $k$ ) of 0.85, obtained from research by (Chianucci, 2020). The data generated from the testing will be subjected to linear regression to obtain slope, intercept, R squared, Mean Absolute Error (Sammut and Webb, 2017), and Root Mean Square Error values (Dua et al., 2017).

### 3. Result and Discussion

The results from Gap Fraction estimation are presented in Table 3. Versions 0 and 1 exhibit slope values close to 1 (Figure 8), akin to the CaCo and coverR methods utilized as references. This suggests that these methods demonstrate good agreement with the TLS-derived results. Despite versions 0, 1, and 2 showing higher error values, the



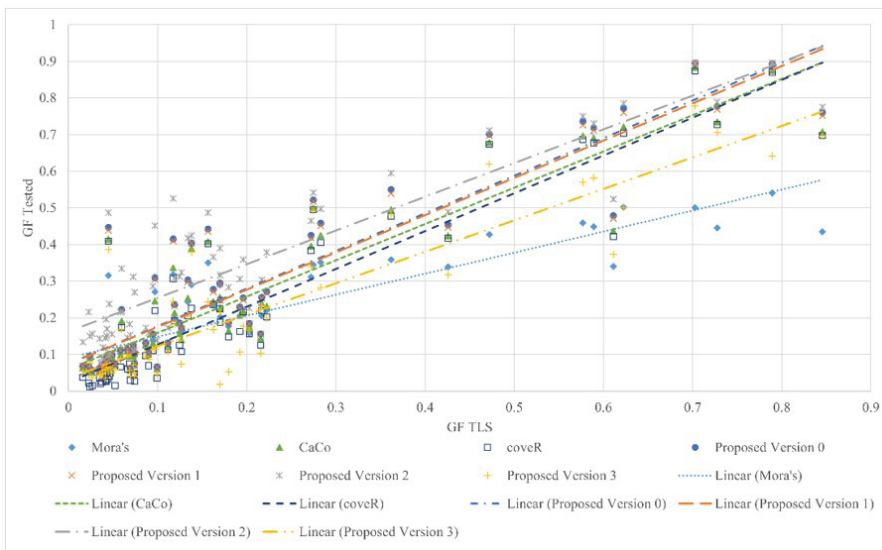
**Figure 7.** Combined result for Version 3.

discrepancy in slope values suggests that Mora's method excels in estimating small Gap Fraction values. However, since the dataset pre-dominantly comprises small Gap Fraction values, the method yields slightly lower errors. As depicted in Figure 9, Mora's method exhibits lower errors at small Gap Fraction values. Nevertheless, as the Gap Fraction value increases, the resulting estimations are lower than those of the proposed method, as indicated by the slope. This discrepancy may stem from the shortcomings in the second segmentation result of Mora's method, which have been rectified in version 0 of this study.

In Version 1, a slight reduction in overestimation compared to Version 0 is evident, reflected in the lower slope value. This reduction is achieved by minimizing the amount of wood through filtering, consequently increasing the denominator. However, Versions 2 and 3 tend to

**Table 3.** Gap Fraction estimation result.

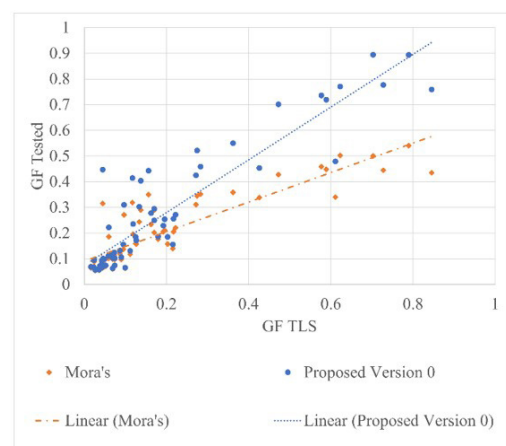
Method	References	Slope	Intercept	R <sup>2</sup>	RMSE	MAE
Mora	Mora et al. (2016)	0.5741	0.0906	0.7677	0.1125	0.0754
CaCo	Alivernini et al. (2018)	0.9897	0.06	0.8498	0.1054	0.0734
coveR	Chianucci et al. (2022)	1.0317	0.0238	0.8566	0.0944	0.0603
Proposed Method Version 0		1.0268	0.0741	0.8415	0.1233	0.0900
Proposed Method Version 1		1.0167	0.0731	0.8422	0.1204	0.0877
Proposed Method Version 2		0.9205	0.1619	0.7978	0.1770	0.1514
Proposed Method Version 3		0.8589	0.0364	0.8174	0.0914	0.0594

**Figure 8.** Gap Fraction estimation result from all tested methods. Line shows linear regression result for each method.

underestimate Gap Fraction based on regression results. Despite Version 3 yielding the lowest Root Mean Square Error (RMSE) and Mean Absolute Error (MAE) values, approaching those obtained using the CoveR method, Version 2 exhibits the most prominent error value among all methods.

A similar trend is observed in LAI estimation, where Versions 0, 1, and 3 show improvement compared to the baseline method, evident from the resulting slope value in Table 4. However, Version 2 demonstrates a poorer slope value compared to the baseline method and exhibits the highest error, contrasting with Version 3, which records the smallest error value among all tested methods, mirroring the results of Gap Fraction estimation. However, due to the difference in field of view (FOV) between the TLS instrument and the Digital Cover Photography (DCP), where TLS has a broader FOV, none of the methods yield values that are very close.

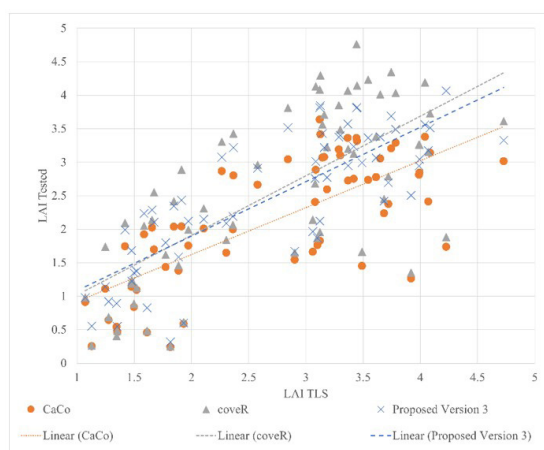
All mentioned methods can be categorized into two groups based on the assumption of LAI used. The first group assumes LAI consists only of leaves or green parts of the plant. The Mora method, Versions 0, 1, and 2 fall into this

**Figure 9.** Gap Fraction estimation result from Mora's and Proposed Method Version 0.

first group. The second group assumes that non-leaf parts, such as wood, are included in LAI calculation, considering

**Table 4.** Leaf Area Index estimation result.

Method	References	Slope	Intercept	R <sup>2</sup>	RMSE	MAE
Mora	Mora et al. (2016)	0.5741	0.0906	0.7677	0.1125	0.0754
CaCo	Alivernini et al. (2018)	0.9897	0.06	0.8498	0.1054	0.0734
coverR	Chianucci et al. (2022)	1.0317	0.0238	0.8566	0.0944	0.0603
Proposed Method Version 0		1.0268	0.0741	0.8415	0.1233	0.0900
Proposed Method Version 1		1.0167	0.0731	0.8422	0.1204	0.0877
Proposed Method Version 2		0.9205	0.1619	0.7978	0.1770	0.1514
Proposed Method Version 3		0.8589	0.0364	0.8174	0.0914	0.0594

**Figure 10.** LAI estimation result from CaCo, coverR and Proposed Method Version 3.

that leaves often cover the wood (Ariza-Carricondo et al., 2019), also referred to as Plant Area Index (Fang et al., 2019). CaCo, coverR, and Version 3 methods belong to this second group. The data obtained using TLS equipment also falls into the second group. Therefore, it is inconclusive whether Versions 0, 1, and 2 are superior to the Mora et al. method due to the absence of datasets comprising only green parts.

In the second group, Version 3 demonstrated improvement by achieving a lower error value compared to the CaCo and coverR methods in both Gap Fraction and Leaf Area Index estimation values. This improvement resulted from Version 3 providing estimation values that were closer to the actual values, as depicted in Figure 10, whereas the other two methods produced more scattered estimation results. Despite Version 3 requiring more complex computation due to different segmentation stages, modern computing capabilities should minimize any impact on performance.

Nevertheless, it is crucial to acknowledge the limitations of this study. The findings are based on a specific dataset using digital cover photography and may not be generalizable to all forest types. Moreover, comparisons with existing methods are constrained by differences in methodology and assumptions. Further research with larger and more diverse datasets is essential to validate and extend these findings.

## 4. Conclusion

Currently, there is a lack of readily available applications for estimating Leaf Area Index while considering the brown color of the image. Given limitations identified in the base method, enhancements were introduced to the proposed method, resulting in three different versions. Among these, Version 3 demonstrated superior performance compared to CaCo and coverR methods, exhibiting lower errors in estimating both Gap Fraction and Leaf Area Index. However, Version 3 entails increased computational complexity due to an additional segmentation step. Owing to the absence of datasets considering LAI solely as the green parts of plants, it remains inconclusive whether the proposed Version 0, 1, and 2 methods outperform the base method. Consequently, further testing using datasets that exclusively consider green leaf parts in estimating LAI values is imperative. Precise LAI estimation has a direct impact on calculating photosynthesis rates and helps assess the forest's capacity to absorb and store carbon dioxide, contributing to climate change mitigation. As a next step, we aim to implement this method in a web-based application to enhance monitoring effectiveness, facilitating broader application and utilization of our research findings in practical environmental management scenarios.

## Acknowledgements

The authors gratefully acknowledge financial support from the Institut Teknologi Sepuluh Nopember for this work, under project scheme of the Publication Writing and IPR Incentive Program (PPHKI) 2023.

## References

- ALIVERNINI, A., FARES, S., FERRARA, C. and CHIANUCCI, F., 2018. An objective image analysis method for estimation of canopy attributes from digital cover photography. *Trees (Berlin)*, vol. 32, no. 3, pp. 713-723. <http://doi.org/10.1007/s00468-018-1666-3>.
- ARIZA-CARRICONDO, C., DI MAURO, F., DE BEECK, M.O., ROLAND, M., GIELEN, B., VITALE, D., CEULEMANS, R. and PAPAIE, D., 2019. A comparison of different methods for assessing leaf area index in four canopy types. *Lesnický Casopis*, vol. 65, no. 2, pp. 67-80. <http://doi.org/10.2478/forj-2019-0011>.
- BECKSCHÄFER, P., SEIDEL, D., KLEINN, C. and XU, J., 2013. On the exposure of hemispherical photographs in forests. *IForest*

- (*Viterbo*), vol. 6, no. 4, pp. 228-237. <http://doi.org/10.3832/ifer0957-006>.
- CASA, R., UPRETI, D. and PELOSI, F., 2019. Measurement and estimation of leaf area index (LAI) using commercial instruments and smartphone-based systems. *IOP Conference Series. Earth and Environmental Science*, vol. 27, no. 1, pp. 012006. <http://doi.org/10.1088/1755-1315/275/1/012006>.
- CHIANUCCI, F. and CUTINI, A., 2012. Digital hemispherical photography for estimating forest canopy properties: current controversies and opportunities. *IForest (Viterbo)*, vol. 5, no. 6, pp. 290-295. <http://doi.org/10.3832/ifer0775-005>.
- CHIANUCCI, F., 2015. A note on estimating canopy cover from digital cover and hemispherical photography. *Silva Fennica*, vol. 50, no. 1. <http://doi.org/10.14214/sf.1518>.
- CHIANUCCI, F., 2020. An overview of in situ digital canopy photography in forestry. *Canadian Journal of Forest Research*, vol. 50, no. 3, pp. 227-242. <http://doi.org/10.1139/cjfr-2019-0055>.
- CHIANUCCI, F., FERRARA, C. and PULETTI, N., 2022. cov-eR: an R package for processing Digital Cover Photography images to retrieve forest canopy attributes. *Trees (Berlin)*, vol. 36, no. 6, pp. 1933-1942. <http://doi.org/10.1007/s00468-022-02338-5>.
- DE BEI, R., FUENTE, S., GILLIHAM, M., TYERMAN, S., EDWARDS, E., BIANCHINI, N., SMITH, J. and COLLINS, C., 2016. VitiCanopy: a free computer app to estimate canopy vigor and porosity for grapevine. *Sensors (Basel)*, vol. 16, no. 4, pp. 585. <http://doi.org/10.3390/s16040585>. PMID:27120600.
- DUA, R., GHOTRA, M.S. and PENTREATH, N., 2017. *Machine learning with spark*. 2nd ed. Birmingham: Packt Publishing.
- FANG, H., BARET, F., PLUMMER, S. and SCHAEPMAN-STRUB, G., 2019. An overview of global Leaf Area Index (LAI): methods, products, validation, and applications. *Reviews of Geophysics*, vol. 57, no. 3, pp. 739-799. <http://doi.org/10.1029/2018RG000608>.
- FUENTES, S., PALMER, A.R., TAYLOR, D., ZEPPEL, M., WHITLEY, R. and EAMUS, D., 2008. An automated procedure for estimating the leaf area index (LAI) of woodland ecosystems using digital imagery, MATLAB programming and its application to an examination of the relationship between remotely sensed and field measurements of LAI. *Functional Plant Biology*, vol. 35, no. 10, pp. 1070-1079. <http://doi.org/10.1071/FP08045>. PMID:32688855.
- JENNINGS, S.B., BROWN, N.D. and SHEIL, D., 1999. Assessing forest canopies and understorey illumination: canopy closure, canopy cover and other measures. *Forestry*, vol. 72, no. 1, pp. 59-73. <http://doi.org/10.1093/forestry/72.1.59>.
- JOHANSSON, T., 1985. Estimating canopy density by the vertical tube method. *Forest Ecology and Management*, vol. 11, no. 1, pp. 139-144. [http://doi.org/10.1016/0378-1127\(85\)90063-5](http://doi.org/10.1016/0378-1127(85)90063-5).
- LIU, J., LI, L., AKERBLUM, M., WANG, T., SKIDMORE, A., ZHU, X. and HEURICH, M., 2021. Comparative evaluation of algorithms for Leaf Area Index Estimation from digital hemispherical photography through virtual forests. *Remote Sensing (Basel)*, vol. 13, no. 16, pp. 3325. <http://doi.org/10.3390/rs13163325>.
- MACFARLANE, C., HOFFMAN, M., EAMUS, D., KERP, N., HIGGINSON, S., MCMURTRIE, R. and ADAMS, M., 2007. Estimation of leaf area index in eucalypt forest using digital photography. *Agricultural and Forest Meteorology*, vol. 143, no. 3-4, pp. 176-188. <http://doi.org/10.1016/j.agrformet.2006.10.013>.
- MORA, M., AVILA, F., CARRASCO-BENAVIDES, M., MALDONADO, G., OLGUÍN-CÁCERES, J. and FUENTES, S., 2016. Automated computation of leaf area index from fruit trees using improved image processing algorithms applied to canopy cover digital photographs. *Computers and Electronics in Agriculture*, vol. 123, pp. 195-202. <http://doi.org/10.1016/j.compag.2016.02.011>.
- NOMURA, K., TAKADA, A., KUNISHIGE, H., OZAKI, Y., OKAYASU, T., YASUTAKE, D. and KITANO, M., 2020. Long-term and continuous measurement of canopy photosynthesis and growth of spinach. *Environment Control in Biology*, vol. 58, no. 2, pp. 21-29. <http://doi.org/10.2525/ecb.58.21>.
- PARKER, G.G., 2020. Tamm review: leaf Area Index (LAI) is both a determinant and a consequence of important processes in vegetation canopies. *Forest Ecology and Management*, vol. 477, pp. 118496. <http://doi.org/10.1016/j.foreco.2020.118496>.
- RANI, P.L., SREENIVAS, G. and REDDY, D.R., 2016. Calibration and validation of CERES-maize model for hybrid maize under variable plant densities and nitrogen levels in Southern Telangana Zone of Telangana State, India. *International Journal of Bio-Resource and Stress Management*, vol. 7, no. 2, pp. 212-217. <http://doi.org/10.23910/IJBMS/2016.7.2.1533>.
- SAMMUT, C. and WEBB, G.I., 2017. Mean absolute error. In: C. SAMMUT and G.I. WEBB, eds. *Encyclopedia of machine learning and data mining*. Boston: Springer. [http://doi.org/10.1007/978-1-4899-7687-1\\_953](http://doi.org/10.1007/978-1-4899-7687-1_953).
- SMAGIN, A.V., SADOVNIKOVA, N.B., BELYAEVA, E.A., KORCHAGINA, K.V. and KRIVTSOVA, V.N., 2023. Simulation modeling and practical use of the hydrological function of detritus in soil engineering technologies. *Moscow University Soil Science Bulletin*, vol. 78, no. 4, pp. 396-409. <http://doi.org/10.3103/S0147687423040075>.
- STUART-HAËNTJENS, E.J., CURTIS, P.S., FAHEY, R.T., VOGEL, C.S. and GOUGH, C.M., 2015. Net primary production of a temperate deciduous forest exhibits a threshold response to increasing disturbance severity. *Ecology*, vol. 96, no. 9, pp. 2478-2487. <http://doi.org/10.1890/14-1810.1>. PMID:26594704.
- XU, X., XU, S., JIN, L. and SONG, E., 2011. Characteristic analysis of Otsu threshold and its applications. *Pattern Recognition Letters*, vol. 32, no. 7, pp. 956-961. <http://doi.org/10.1016/j.patrec.2011.01.021>.